ChemComm

COMMUNICATION

View Article Online
View Journal | View Issue

Cite this: *Chem. Commun.*, 2024, **60**, 15019

Received 9th October 2024,
Accepted 11th November 2024

DOI: 10.1039/d4cc05214e

rsc.li/chemcomm

Endosomolytic peptides enable the cellular delivery of peptide nucleic acids†

JoLynn B. Giancola and Ronald T. Raines *

Precision genetic medicine enlists antisense oligonucleotides (ASOs) to bind to nucleic acid targets important for human disease. Peptide nucleic acids (PNAs) have many desirable attributes as ASOs but lack cellular permeability. Here, we use an assay based on the corrective splicing of an mRNA to assess the ability of synthetic peptides to deliver a functional PNA into a human cell. We find that the endosomolytic peptides L17E and L17ER$_4$ are highly efficacious delivery vehicles. Co-treatment of a PNA with low micromolar L17E or L17ER$_4$ enables robust corrective splicing in nearly all treated cells. Peptide–PNA conjugates are even more effective. These results enhance the utility of PNAs as research tools and potential therapeutic agents.

Oligonucleotides have garnered enormous attention for their therapeutic potential. Eighteen nucleic acid-based drugs are on the market, and dozens more are in clinical development.[1] Because oligonucleotide-target engagement is governed by Watson–Crick–Franklin base pairing, therapeutic oligonucleotides can easily be designed to have high target specificity, obviating the need for the iterative screening required to develop small-molecule therapies.[2]

Antisense oligonucleotides (ASOs) leverage mRNA binding as a means to control protein levels in a cell.[3,4] Upon binding to an mRNA target in the cytosol, an ASO can induce target degradation. Alternatively, binding to an mRNA target in the nucleus can direct splicing that enables (or disables) its translation.

Peptide nucleic acids (PNAs) are heralded ASOs in which the ribose phosphate backbone of an oligonucleotide is replaced with one that is peptidic in nature.[5] PNAs have exquisite specificity for their complementary nucleic acid and bind with higher affinity than do their DNA counterparts because their neutral backbone obviates the Coulombic repulsion endemic in double-stranded nucleic acids.[6,7] PNAs are achiral and readily accessible by solid-phase synthesis methods akin to those for accessing peptides.[8] Moreover, PNAs are highly stable under physiological conditions and not known to be immunogenic. These attributes have made the application of PNAs in the laboratory and clinic of special interest.[9,10]

To function in a live cell, a PNA must enter the cytosol. PNAs are, however, unable to penetrate the plasma membrane of mammalian cells. Their ability to access the cytosol is notoriously inefficient, even with delivery vehicles.[2,11–21] Accordingly, the utility of PNAs has been constrained since their invention over thirty years ago.[5]

In 2017, Futaki and coworkers reported on L17E, an endosomolytic peptide derived from M-lycotoxin.[22] This peptide affords cytosolic access to cargo through endosomal membrane rupture after macropinocytotic uptake.[23] L17E has been employed primarily as a co-treatment agent in protein delivery experiments.[24] Only a few reports disclose the use of this peptide as a covalent appendage for the delivery of oligonucleotides.[25,26] In 2022, the Futaki group reported that a pendant arginine-rich sequence makes L17E even more effective for the cellular delivery of proteinaceous cargo.[27]

Here, we assess the efficiency of PNA delivery into human cells as mediated by three peptides: L17E,[22] L17ER$_4$ (which contains four arginine residues),[27] and R10 (which is a well-known cell-penetrating peptide).[28] To assess delivery, we employ a rigorous quantitative assay based on the corrective splicing of an mRNA that is translated into the green fluorescent protein (GFP) (Scheme 1). First, we compare the cellular uptake of a PNA upon co-treatment with each peptide. Then, we explore the delivery efficiency upon conjugation of the peptide to the PNA. We find that endosomolytic peptides can effect the highly efficient delivery of a PNA into human cells.

Our first goal was to demonstrate the cytosolic delivery of a PNA into human cells. For this purpose, we chose to deliver PNA654, which can orchestrate the corrective splicing of a GFP pre-mRNA in an engineered human cell line (HeLa654), resulting in the production of GFP.[29–32] This assay enabled us to make comparisons between different treatment conditions because GFP fluorescence reports directly on the delivery of a functional PNA (Scheme 1). We used standard solid-phase methods to synthesize the necessary peptides (Scheme 2). In some peptides, azido groups enable strain-promoted azide–alkyne cycloaddition (SPAAC) for subsequent conjugation.

We were aware that cell-penetrating peptides can diminish cell viability.[28] Accordingly, we treated HeLa654 cells with R10, L17E, or

Department of Chemistry, Massachusetts institute of Technology, 77 Massachusetts Avenue, Cambridge, MA 02139, USA. E-mail: rtraines@mit.edu

† Electronic supplementary information (ESI) available. See DOI: https://doi.org/10.1039/d4cc05214e

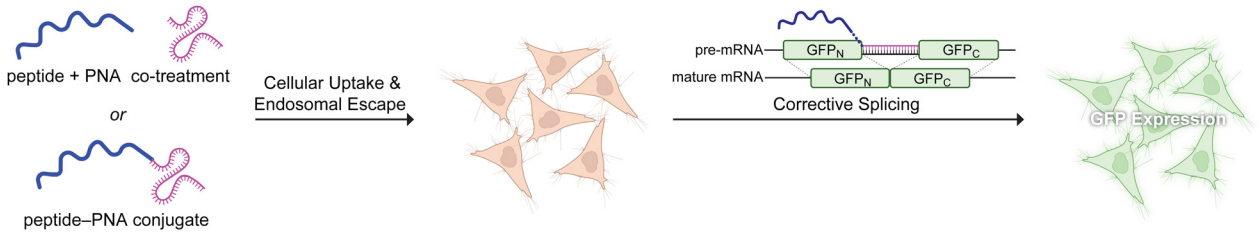

Scheme 1 Assay for the delivery of a functional PNA into live human cells.

L17ER$_4$ and assessed their viability with a tetrazolium-based assay[33] and their morphology with epifluorescence microscopy. R10 and L17E did not have a detectable effect on viability at all assayed concentrations (Fig. S16, ESI†). In contrast, L17ER$_4$ was cytotoxic above 5 μM in the absence of serum and above 20 μM in the presence of serum. These data were consistent with morphological assessments (Fig. S17, ESI†) and guided subsequent experiments.

Next, we characterized the cellular uptake of the endosomolytic peptides. To do so, we used SPAAC to link an azido group installed at the N or C terminus with the strained alkynyl group of TAMRA-DBCO. These conjugates also served as proxies for conjugates to larger biomolecules.[27] Upon incubation with human cells, we found that modification of the endosomolytic peptides at their C terminus led to greater cellular uptake (Fig. 1). Hence, the C terminus was used as the premier conjugation site in all future experiments. Guided by data with TAMRA-labelled peptides, we used SPAAC to prepare the R10–PNA, L17E–PNA, and L17ER$_4$–PNA conjugates in which the PNA is installed at the C terminus of the peptide.

To evaluate the cellular delivery of a PNA, we treated HeLa654 cells with PNA/peptide constructs for 5–7 min in Dulbecco's modified Eagle's medium (DMEM) without serum or 1 h in complete medium. These conditions were guided by cellular viability (Fig. S16, ESI†) and literature precedent.[27] After treatment, the cells were washed with phosphate-buffered saline and permitted to recover for an additional 27 h in complete medium in a humidified incubator at 37 °C prior to epifluorescence imaging.

Our initial PNA delivery experiments focused on the utility of a co-treatment with R10, L17E, and L17ER$_4$. In these serum-free experiments, we used R10, L17E, and L17ER$_4$ at 40, 40, and 20 μM, respectively, and PNA at 1–30 μM. Without a peptide or with R10, we observed only modest GFP production, indicative of little cellular uptake (Fig. 2 and 3). In contrast, we observed substantial fluorescence with 40 μM L17E and, even more so, with 20 μM L17ER$_4$ (Fig. 2). Interestingly, and in contrast to our cytotoxicity data, we observed mild toxicity for cells treated with 20 μM L17ER$_4$ and low PNA concentrations (1 and 5 μM), but abrogation of this cytotoxicity with high PNA concentrations (15 and 30 μM). These data suggest that a nearly stoichiometric peptide : PNA ratio is desirable for co-treatments with L17ER$_4$ and motivated us to assess a covalent 1 : 1 conjugate of the peptide and PNA.

Before testing peptide–PNA conjugates, we probed for an effect of the cell cycle on PNA delivery. To do so, we synchronized

Peptides

R10	H-**RRRRRRRRRR**-NH_2
azide-R10	$N_3(CH_2)_4C(O)[NH(CH_2)_2O(CH_2)_2OCH_2C(O)]_2$-**RRRRRRRRRR**-$NH_2$
L17E	H-**IWLTALKFLGKHAAKHEAKQQLSKL**-NH_2
azide-L17E	H-**K**(N_3)**GGIWLTALKFLGKHAAKHEAKQQLSKL**-NH_2
L17E-azide	H-**IWLTALKFLGKHAAKHEAKQQLSKLGGK**(N_3)-NH_2
L17ER$_4$	H-**IWLTALKFLGKHAAKHEAKQQLSKLGRRRR**-NH_2
azide-L17ER$_4$	H-**K**(N_3)**GGIWLTALKFLGKHAAKHEAKQQLSKLGRRRR**-NH_2
L17ER$_4$-azide	H-**IWLTALKFLGKHAAKHEAKQQLSKLGRRRRGGK**(N_3)-NH_2

Fluorophore

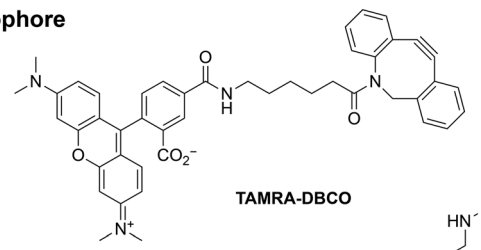

PNAs

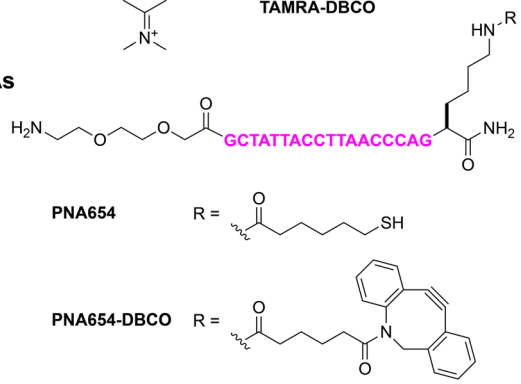

Scheme 2 Molecules used in this work.

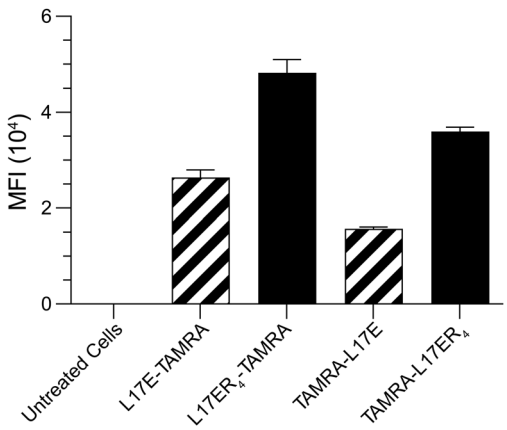

Fig. 1 Graph of the mean fluorescence intensities (MFIs) from TAMRA-labelled L17E and L17ER$_4$ in human cells. HeLa654 cells were treated for 5 min with peptides (5 μM) labelled at their N or C terminus in medium without serum, allowed to recover for 1 h in complete medium, and assessed with flow cytometry. For experimental conditions and representative flow cytometry plots, see Table S2, Fig. S18, and S19 (ESI).†

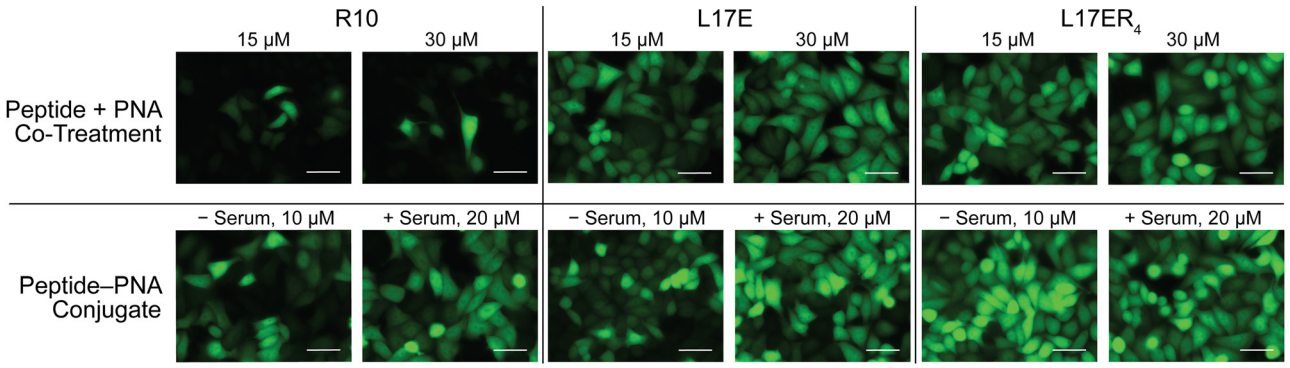

Fig. 2 Microscopy images of GFP in human cells produced upon corrective splicing by a PNA delivered with peptide co-treatment or conjugation (Scheme 1). Experimental conditions and additional images are provided in Table S3 (ESI).† Standardized laser intensities were normalized across all treatment conditions. Additional images are shown in Fig. S23, S25, S28, S30, S32, and S34 (ESI).† Scale bars: 50 μM.

cells by using RO-3306, which is a small-molecule CDK1 inhibitor that arrests the cell cycle at the G2/M phase boundary.[34] We chose that point in the cell cycle because of the known increase in ceramide concentration in membranes there,[35,36] the role of ceramides in forming nucleation zones that direct endocytosis,[37–41] and the correlation between improved cargo uptake in dividing cells.[42] Cells were seeded at equivalent densities, and a subset was synchronized by the addition of RO-3306 (9 μM for 20 h). To ensure that we captured cells after their re-entry into the cell cycle but while they were dividing, we administered L17E and the PNA immediately following the withdrawal of RO-3306, using a 2-h treatment window in complete medium. We observed that synchronizing cells did not potentiate GFP production (Fig. S36 and S37, ESI†), suggesting that ceramides are not involved in the uptake mechanism.

Next, we discerned whether covalently linking a peptide to the PNA was beneficial to cellular uptake. Specifically, we treated HeLa654 cells with peptide–PNA conjugates either at 5 and 10 μM for 7 min in DMEM without serum or at 10 and 20 μM for 1 h in complete medium. We observed a marked enhancement in performance by R10 when covalently attached to the PNA (Fig. 2). Still, both endosomolytic peptides outperformed R10. Moreover, GFP production appeared to be greater from $L17ER_4$–PNA than from L17E–PNA in the absence or presence of serum (Fig. 2).

Finally, we used flow cytometry to quantify the cellular GFP induced by a PNA upon co-treatment or conjugation. Consistent with our imaging analysis, co-treatment with R10 affords little GFP (Fig. 3 and Fig. S29, ESI†). In contrast, we found a robust dose-dependent response for GFP production upon co-treatment with endosomolytic peptides (Fig. 3 and Fig. S24 and S26, ESI†). At 1 μM, $L17ER_4$ and L17E elicit PNA function to a similar extent, but $L17ER_4$ elicits more function than L17E at concentrations ≥ 5 μM. Notably, we found that at PNA concentrations of 15 and 30 μM, both L17E and $L17ER_4$ enable $>90\%$ of cells to be transfected successfully with the PNA (Fig. S24 and S26, ESI†). Even at 5 μM $L17ER_4$, $>85\%$ of cells produce GFP (Fig. S26, ESI†). Overall, co-treatment with L17E or $L17ER_4$ gives a 23- or 27-fold increase, respectively, in GFP expression (Fig. 3).

A covalent linkage with a peptide enhances the function of the PNA in cells (Fig. 3). Under each condition, the GFP levels induced by a conjugate exceeded that obtained with co-treatment. Oftentimes, the cellular delivery of cargo is dampened by the addition of serum because of nonspecific adsorption of the cargo to serum proteins.[43] In marked contrast, the intracellular delivery of PNA conjugates with endosomolytic peptides was potentiated in serum, likely due to the increase in incubation time. Moreover, treatment conditions with L17E

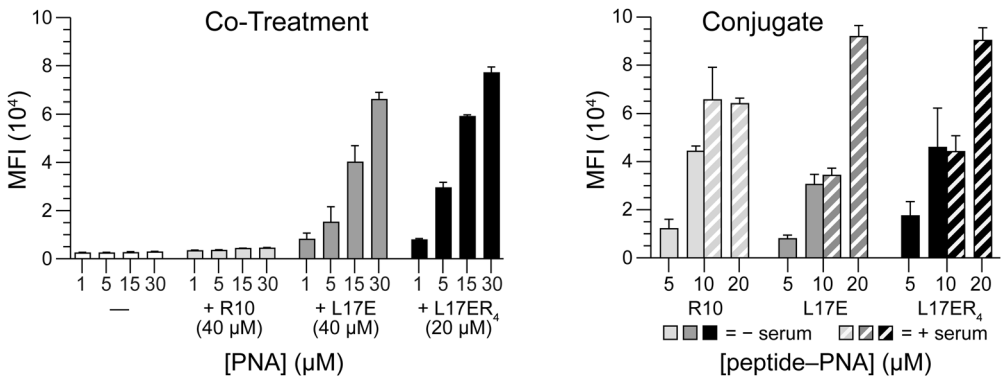

Fig. 3 Graphs of MFIs from GFP in human cells produced upon corrective splicing by a PNA delivered with peptide co-treatment or conjugation (Scheme 1). Serum-free conditions were used for co-treatment. For additional experimental conditions and representative flow cytometry plots, see Table S3, Fig. S21, S22, S24, S26, S29, S31, S33, and S35 (ESI).† Standardized laser intensities were used across all experiments.

and L17ER$_4$ can enable ~95% of cells to produce GFP (Fig. S31 and S33, ESI†). Conjugation further potentiates GFP expression over PNA alone, with a 32- or 37-fold increase in fluorescence for L17E or L17ER$_4$, respectively (Fig. 3). These expression levels compare favourably with other preeminent ASO delivery strategies using this exact assay.[25,30–32]

In conclusion, we have found that the endosomolytic peptides L17E and L17ER$_4$ are highly efficacious and superior to R10 in effecting the delivery of a functional PNA into a human cell. Unlike previous delivery strategies for antisense therapeutics, nearly all cells produce GFP after either co-treatment with low micromolar concentrations of L17E or L17ER$_4$ or conjugation to these peptides.[16,25,30] L17E affords robust cellular uptake without compromising cell viability, with less efficacy than L17ER$_4$. The co-treatment strategy is an especially facile means to deliver a PNA into a human cell *in vitro*, whereas conjugation has the potential for use *in vivo* and could enable clinical translation. We anticipate that our findings will enhance the utility of PNAs and other ASOs in a wide variety of applications.

The authors are grateful to Dr C. K. Schissel and Prof. B. L. Pentelute for providing the HeLa654 cell line. They thank the Koch Institute's Robert A. Swanson (1969) Biotechnology Center for technical support, specifically the High Throughput Sciences core for mycoplasma testing. They are grateful to Dr J. Yang, Dr E. C. Wralstad, and N. R. F. Knowles for helpful discussions. Some figures were created with BioRender. This work was supported by Grants R35 GM148220 and P30 CA014051 (NIH).

Data availability

The data supporting this article have been included in the ESI.†

Conflicts of interest

There are no conflicts to declare.

Notes and references

1 M. Egli and M. Manoharan, *Nucleic Acids Res.*, 2023, **51**, 2529–2573.
2 T. C. Roberts, R. Langer and M. J. A. Wood, *Nat. Rev. Drug Discovery*, 2020, **19**, 673–694.
3 A. Amantana, H. M. Moulton, M. L. Cate, M. T. Reddy, T. Whitehead, J. N. Hassinger, D. S. Youngblood and P. L. Iversen, *Bioconjugate Chem.*, 2007, **18**, 1325–1331.
4 K. Dhuri, C. Bechtold, E. Quijano, H. Pham, A. Gupta, A. Vikram and R. Bahal, *J. Clin. Med.*, 2020, **9**, 2004.
5 M. Egholm, O. Buchardt, P. E. Nielsen and R. H. Berg, *J. Am. Chem. Soc.*, 1992, **114**, 1895–1897.
6 M. Egholm, O. Buchardt, L. Christensen, C. Behrens, S. M. Freier, D. A. Driver, R. H. Berg, S. K. Kim, B. Norden and P. E. Nielsen, *Nature*, 1993, **365**, 566–568.
7 P. Wittung, P. E. Nielsen, O. Buchardt, M. Egholm and B. Norden, *Nature*, 1994, **368**, 561–563.
8 K. Klabenkova, A. Fokina and D. Stetsenko, *Molecules*, 2021, **26**, 5420.
9 S. Montazersaheb, M. S. Hejazi and H. Nozad Charoudeh, *Adv. Pharm. Bull.*, 2018, **8**, 551–563.
10 N. Brodyagin, M. Katkevics, V. Kotikam, C. A. Ryan and E. Rozners, *Beilstein J. Org. Chem.*, 2021, **17**, 1641–1688.
11 U. Koppelhus and P. E. Nielsen, *Adv. Drug Delivery Rev.*, 2003, **55**, 267–280.
12 K. Kaihatsu, K. E. Huffman and D. R. Corey, *Biochemistry*, 2004, **43**, 14340–14347.
13 J. J. Turner, G. D. Ivanova, B. Verbeure, D. Williams, A. A. Arzumanov, S. Abes, B. Lebleu and M. J. Gait, *Nucleic Acids Res.*, 2005, **33**, 6837–6849.
14 S. Abes, D. Williams, P. Prevot, A. Thierry, M. J. Gait and B. Lebleu, *J. Controlled Release*, 2006, **110**, 595–604.
15 N. Spinelli, E. Defrancq and F. Morvan, *Chem. Soc. Rev.*, 2013, **42**, 4557–4573.
16 C. Cordier, F. Boutimah, M. Bourdeloux, F. Dupuy, E. Met, P. Alberti, F. Loll, G. Chassaing, F. Burlina and T. E. Saison-Behmoaras, *PLoS One*, 2014, **9**, e104999.
17 J. Saarbach, P. M. Sabale and N. Winssinger, *Curr. Opin. Chem. Biol.*, 2019, **52**, 112–124.
18 M. Ghavami, T. Shiraishi and P. E. Nielsen, *Biomolecules*, 2019, **9**, 554.
19 T. Shiraishi, M. Ghavami and P. E. Nielsen, *Methods Mol. Biol.*, 2020, **2105**, 173–185.
20 J. A. Kulkarni, D. Witzigmann, S. B. Thomson, S. Chen, B. R. Leavitt, P. R. Cullis and R. van der Meel, *Nat. Nanotechnol.*, 2021, **16**, 630–643.
21 Ö. Öztürk, A.-L. Lessl, M. Höhn, S. Wuttke, P. E. Nielsen, E. Wagner and U. Lächelt, *Sci. Rep.*, 2023, **13**, 14222.
22 M. Akishiba, T. Takeuchi, Y. Kawaguchi, K. Sakamoto, H. H. Yu, I. Nakase, T. Takatani-Nakase, F. Madani, A. Gräslund and S. Futaki, *Nat. Chem.*, 2017, **9**, 751–761.
23 M. Akishiba and S. Futaki, *Mol. Pharm.*, 2019, **16**, 2540–2548.
24 J. B. Giancola, J. B. Grimm, J. V. Jun, Y. D. Petri, L. D. Lavis and R. T. Raines, *ACS Chem. Biol.*, 2024, **19**, 908–915; and references therein.
25 B. Becker, S. Englert, H. Schneider, D. Yanakieva, S. Hofmann, C. Dombrowsky, A. Macarrón Palacios, S. Bitsch, A. Elter, T. Meckel, B. Kugler, A. Schirmacher, O. Avrutina, U. Diederichsen and H. Kolmar, *J. Peptide Sci.*, 2021, **27**, e3298.
26 R. Feng, R. Ni and Y. Chau, *Biomater. Sci.*, 2022, **10**, 5116–5120.
27 K. Shinga, T. Iwata, K. Murata, Y. Daitoku, J. Michibata, J. V. V. Arafiles, K. Sakamoto, M. Akishiba, T. Takatani-Nakase, S. Mizuno, F. Sugiyama, M. Imanishi and S. Futaki, *Bioorg. Med. Chem.*, 2022, **61**, 116728.
28 P. G. Dougherty, A. Sahni and D. Pei, *Chem. Rev.*, 2019, **119**, 10241–10287.
29 P. Sazani, S.-H. Kang, M. A. Maier, C. Wei, J. Dillman, J. Summerton, M. Manoharan and R. Kole, *Nucleic Acids Res.*, 2001, **29**, 3965–3974.
30 J. M. Wolfe, C. M. Fadzen, Z.-N. Choo, R. L. Holden, M. Yao, G. J. Hanson and B. L. Pentelute, *ACS Cent. Sci.*, 2018, **4**, 512–520.
31 C. K. Schissel, S. Mohapatra, J. M. Wolfe, C. M. Fadzen, K. Bellovoda, C. L. Wu, J. A. Wood, A. B. Malmberg, A. Loas, R. Gómez-Bombarelli and B. L. Pentelute, *Nat. Chem.*, 2021, **13**, 992–1000.
32 C. Li, A. J. Callahan, K. S. Phadke, B. Bellaire, C. E. Farquhar, G. Zhang, C. K. Schissel, A. J. Mijalis, N. Hartrampf, A. Loas, D. E. Verhoeven and B. L. Pentelute, *ACS Cent. Sci.*, 2022, **8**, 205–213.
33 A. H. Cory, T. C. Owen, J. A. Barlrop and J. G. Cory, *Cancer Commun.*, 1991, **3**, 207–212.
34 L. T. Vassilev, C. Tovar, S. Chen, D. Knezevic, X. Zhao, H. Sun, D. C. Heimbrook and L. Chen, *Proc. Natl. Acad. Sci. U. S. A.*, 2006, **103**, 10660–10665.
35 P. P. Ruvolo, *Leukemia*, 2001, **15**, 1153–1160.
36 M. P. Espaillat, A. A. Shamseddine, M. M. Adada, Y. A. Hannun and L. M. Obeid, *Transl. Cancer Res.*, 2015, **4**, 484–499.
37 F. Duchardt, M. Fotin-Mleczek, H. Schwarz, R. Fischer and R. Brock, *Traffic*, 2007, **8**, 848–866.
38 W. P. R. Verdurmen, M. Thanos, I. R. Ruttekolk, E. Gulbins and R. Brock, *J. Controlled Release*, 2010, **147**, 171–179.
39 A. Sahni, Z. Qian and D. Pei, *ACS Chem. Biol.*, 2020, **15**, 2485–2492.
40 A. F. L. Schneider, M. Kithil, M. C. Cardoso, M. Lehmann and C. P. R. Hackenberger, *Nat. Chem.*, 2021, **13**, 530–539.
41 A. Saha, S. Mandal, J. V. V. Arafiles, J. Gómez-González, C. P. R. Hackenberger and A. Brik, *Angew. Chem., Int. Ed.*, 2022, **61**, e202207551.
42 J. A. Kim, C. Åberg, A. Salvati and K. A. Dawson, *Nat. Nanotechnol.*, 2012, **7**, 62–68.
43 K. Nomura, K. Kawano, Y. Kawaguchi, Y. Kawamura, J. Michibata, K. Kuwata, K. Sugiyama, K. Kusumoto and S. Futaki, *ACS Pharmacol. Transl. Sci.*, 2022, **5**, 603–615.

